Interior tomography from low-count local projections and associated Hilbert transform data

Qiong Xu [a], Hengyong Yu [b,c], Xuanqin Mou [*a], Ge Wang [c,d]
[a]Institute of Image processing and Pattern recognition, Xi'an Jiaotong University, Xi'an, Shaanxi 710049, China;
[b]Dept. of Radiology, Division of Radiologic Sciences, Wake Forest University Health Sciences, Winston-Salem, NC 27157, USA;
[c]Biomedical Imaging Division, VT-WFU School of Biomedical Engineering and Sciences, Wake Forest University Health Sciences, Winston-Salem, NC 27157, USA;
[d]Biomedical Imaging Division, VT-WFU School of Biomedical Engineering and Sciences, Virginia Tech., Blacksburg, VA 24061, USA

ABSTRACT

This paper presents a statistical interior tomography approach combining an optimization of the truncated Hilbert transform (THT) data. With the introduction of the compressed sensing (CS) based interior tomography, a statistical iteration reconstruction (SIR) regularized by the total variation (TV) has been proposed to reconstruct an interior region of interest (ROI) with less noise from low-count local projections. After each update of the CS based SIR, a THT constraint can be incorporated by an optimizing strategy. Since the noisy differentiated back-projection (DBP) and its corresponding noise variance on each chord can be calculated from the Poisson projection data, an object function is constructed to find an optimal THT of the ROI from the noisy DBP and the present reconstructed image. Then the inversion of this optimized THT on each chord is performed and the resulted ROI will be the initial image of next update for the CS based SIR. In addition, a parameter in the optimization of THT step can be used to determine the stopping rule of the iteration heuristically. Numerical simulations are performed to evaluate the proposed approach. Our results indicate that this approach can reconstruct an ROI with high accuracy by reducing the noise effectively.

Keywords: Computed tomography, interior tomography, statistical iteration reconstruction, compressed sensing, truncated Hilbert transform

1. INTRODUCTION

From the conventional CT reconstruction theory, exact image reconstruction requires that the projection data covers the whole imaging object support[1]. Reconstructing an image inside an interior region of interest (ROI) from the truncated projection data along the lines only through the ROI is referred to as interior problem, which can reduce the radiation dose, detector size, imaging duration, and motion artifacts. This kind of imaging model is very useful to local cardiac CT, micro-CT, nano-CT and so on. However, interior problem is not uniquely solvable in mathematics. During these years, many efforts have been devoted to obtain an exact and stable solution for interior problem[2-4].

Recently, it has been proved that interior problem can be exactly solved regularized by some additional information or constraints. This exact-oriented interior reconstruction is named as interior tomography[5]. At present, there are two ingredients for interior tomography. One ingredient is to inverse truncated Hilbert transform (THT) with prior sub-region knowledge, which is called THT-based interior tomography[6-11]. Its main idea is to use the analytic continuation technique to extend the known sub-region to the whole ROI. In its implementation, chords (PI-lines)are defined through the known sub-region, and then the differential backprojection (DBP)[12] operator is performed on each chord, finally the resultant THT is inverted to reconstruct 1D image on each chord by projection on to convex (POCS) or singular value decomposition (SVD). The other is based on compressed sensing (CS) assuming a piecewise constant or polynomial ROI, which is called CS-based interior tomography[13-16]. In light of the CS theory[17], its main idea is to use an appropriate sparsifying transform and an associated objective function to regularize the ambiguity into the null space. In its implementation, the minimization of total variation (TV) or high order TV (HOT) is often adopted. The two

Medical Imaging 2011: Physics of Medical Imaging, edited by Norbert J. Pelc, Ehsan Samei, Robert M. Nishikawa,
Proc. of SPIE Vol. 7961, 796130 · © 2011 SPIE · CCC code: 1605-7422/11/$18 · doi: 10.1117/12.877901

aforementioned interior tomography methods with corresponding priors are theoretically exact[18]. However, the data acquisition process is not deterministic in reality and the noise is unavoidable. And a statistical model can be utilized to describe the physical process.

In order to improve the performance of interior tomography in practice, especially in low-count situation, very recently, we proposed a statistical interior tomography (SIT) method[19, 20]. The CS-based interior tomography is performed in a statistical fashion combining the TV minimization and statistical iterative reconstruction (SIR) framework. Therein, a reconstruction based on the inversion of THT is used as the initial image to enhance the robustness of SIT. The performance of this approach has been validated by both preclinical and clinical experiments. However, in its implementation, the THT constraint is incorporated deterministically without considering its noise property. Moreover, the THT constraint is just used as an initial guess.

In this paper, we propose an improved SIT approach which adds an optimization of THT constraint statistically after each update of the CS based SIR. In the next section, we will describe the proposed algorithm. In section 3, experimental results will be presented. Finally, we will discuss the related problems and conclude the paper in section 4.

2. METHODOLOGY

2.1 Noise in projection and THT

Without loss of generality, we consider the monochromatic x-ray source. And the measured data can be modeled as a Poisson distribution,

$$y_i \sim Poisson\{\bar{y}_i\}, \quad i = 1, \cdots, I, \tag{1}$$

where $\bar{y}_i = b_i e^{-p_i}$ is the expectation of the measurement y_i, b_i the blank scan factor, p_i the linear integral of attenuation coefficients along the x-ray path and I the number of projections. Denote the statistical noise of y_i as n_{y_i}, then $y_i = \bar{y}_i + n_{y_i}$. Due to the Poisson distribution of y_i, we have

$$\mathrm{var}(n_{y_i}) = \bar{y}_i, \ i = 1, \cdots, I. \tag{2}$$

The measured linear integral data is denoted as

$$\hat{p}_i = \ln(b_i / y_i) = p_i + n_{\hat{p}_i}, \ i = 1, \cdots, I, \tag{3}$$

where $n_{\hat{p}_i}$ is the statistical noise of $\hat{p}_i$.

Applying the Taylor's expansion to Eq. (3)[21], there will be

$$\hat{p}_i = \ln b_i - \ln y_i = \ln b_i - \ln(\bar{y}_i + n_{y_i}) = \ln b_i - \ln \bar{y}_i - \frac{n_{y_i}}{\bar{y}_i} + O\left(\left(\frac{n_{y_i}}{\bar{y}_i}\right)^2\right) = p_i - \frac{n_{y_i}}{\bar{y}_i} + O\left(\left(\frac{n_{y_i}}{\bar{y}_i}\right)^2\right), \quad i = 1, \cdots, I. \tag{4}$$

Ignoring the constant and high order terms, the noise variance of $\hat{p}_i$ can be approximated as,

$$\mathrm{var}(n_{\hat{p}_i}) \approx \frac{\mathrm{var}(n_{y_i})}{\bar{y}_i^2} = \frac{1}{\bar{y}_i}, \quad i = 1, \cdots, I. \tag{5}$$

The THT along each chord (PI-line) inside the ROI can be computed using the DBP method, which is a series of weighting, differential, and summation operators on the measured linear integral projections. Therefore, the noise variance of the THT can be easily estimated from the noise variances of $\{\hat{p}_i\}$[22].

2.2 CS based SIR

With the discrete attenuation coefficient on each pixel, the line integral data can be expressed as

$$p_i = \int_{l_i} \mu(\vec{r})\, dl \approx \sum_{j=1}^{J} a_{ij}\mu_j = [\mathbf{A}\boldsymbol{\mu}]_i \ , i = 1, \cdots, I \quad , \tag{6}$$

where $\boldsymbol{\mu} = (\mu_1, \cdots, \mu_J)'$ denotes the linear attenuation coefficient, $\mathbf{A} = \{a_{ij}\}$ the system matrix accounting for imaging geometry and J the number of pixels. Combining the Poisson projection data and TV regularization in the maximization of *a posterior* (MAP) framework, the CS based SIR is to minimize the following objective function[19, 20],

$$\Phi(\boldsymbol{\mu}) = \sum_{i=1}^{I} \frac{y_i}{2}\left([\mathbf{A}\boldsymbol{\mu}]_i - \hat{p}_i\right)^2 + \beta TV(\boldsymbol{\mu}) \, . \tag{7}$$

With the separable paraboloidal surrogate method[23], each update for the log-likelihood term $\sum_{i=1}^{I} \frac{y_i}{2}\left([\mathbf{A}\boldsymbol{\mu}]_i - \hat{p}_i\right)^2$ is obtained as follows,

$$\mu_j^t = \mu_j^{t-1} - \frac{\sum_{i=1}^{I}\left(a_{ij} y_i \left([\mathbf{A}\boldsymbol{\mu}^{t-1}]_i - \hat{p}_i\right)\right)}{\sum_{i=1}^{I}\left(a_{ij} y_i \sum_{k=1}^{J} a_{ik}\right)}, \quad j = 1, \cdots, J \, . \tag{8}$$

We use an alternating minimization method to optimize Eq.(7)[19, 20]. The minimizing steps of the log-likelihood term via Eq. (4) and the TV term via soft-threshold filtration[24] are performed alternately.

2.3 Optimization of THT

On each chord, denote the THT of at a given location in the ROI and its corresponding noise variance as $g^{DBP}(x)$ and $\varepsilon(x)$, where x is the 1-D coordinate along chord. Moreover, the THT along the chord in the ROI can be also computed from an intermediate iterative reconstruction of the CS based SIR denoted as $g^{Old}(x)$.

In a low-count situation, $g^{DBP}(x)$ is more noisy with an unbiased expectation, while $g^{Old}(x)$ is less noisy usually existing a bias. Therefore, we construct the following optimization function to determine the THT along a chord in the ROI, which is denoted as $g^{New}(x)$,

$$\min \Psi\left(g^{New}(x)\right) = \lambda \int \frac{1}{\varepsilon(x)}\left(g^{New}(x) - g^{DBP}(x)\right)^2 dx + \left\| g^{New}(x) - g^{Old}(x) \right\|_2, x \in \Lambda_H \, , \tag{9}$$

where λ is a free parameter, and Λ_H expresses the THT region on each chord. The first term of Eq. (9) is the maximum likelihood estimate (MLE) assuming that $g^{DBP}(x)$ is independent of each other following a Gaussian distribution of variance $\varepsilon(x)$.

Eq.(9) can be discretized as,

$$\min \Psi\left(g_s^{New}\right) = \lambda \sum_s \frac{1}{\varepsilon_s}\left(g_s^{New} - g_s^{DBP}\right)^2 + \sum_s \left(g_s^{New} - g_s^{Old}\right)^2, s \in \Lambda_H \, . \tag{10}$$

Minimizing Eq. (10) leads to the optimized THT,

$$g_s^{New} = g_s^{DBP} + \frac{g_s^{Old} - g_s^{DBP}}{\lambda/\varepsilon_s + 1}, s \in \Lambda_H \, . \tag{11}$$

The parameter λ should satisfy that,

$$\begin{cases} if\ g_s^{Old} \geq g_s^{DBP} + err_s, \quad then\ \dfrac{g_s^{Old} - g_s^{DBP}}{\lambda/\varepsilon_s + 1} \leq err_s \\ if\ g_s^{Old} \leq g_s^{DBP} - err_s, \quad then\ \dfrac{g_s^{Old} - g_s^{DBP}}{\lambda/\varepsilon_s + 1} \geq -err_s \end{cases}, \tag{12}$$

where err_s expresses the estimated uncertainty of g_s^{DBP} which is directly related to ε_s. For simplicity, we choose $err_s = \alpha\sqrt{\varepsilon_s}$ (α is a constant). From Eq. (12), we have

$$\lambda \geq \frac{(P_s - err_s)\varepsilon_s}{err_s}, \quad P_s = \left| g_s^{Old} - g_s^{DBP} \right|. \tag{13}$$

Considering $\lambda \geq 0$, we determine λ heuristically as

$$\lambda = \sum_{s \in \Lambda_H} \max\left\{ \frac{(P_s - err_s)\varepsilon_s}{err_s \sum_{s \in \Lambda_H} 1}, 0 \right\}. \tag{14}$$

When the current THT g^{New} is calculated, its inversion on each chord will lead to a reconstructed result. This result will be the initial image of the next iteration in the CS based SIR step. It can be noticed that: When λ is decreasing, it indicates that the reconstructed result is walking towards the true value and its noise is decreasing. On the other hand, when λ is increasing, it indicates that the reconstructed result is deviating from the best result. Therefore, considering this property of λ, we can stop the iteration when the decreasing of λ becomes slowly or stops.

2.4 Other constraints

Obviously, there are some other constraints irrespective of statistical property, such as,

1). The known sub-region;

2). The support of the imaging object;

3). The non-negativity of the value;

4). The maximum bound of the value.

In every step of reconstruction, we can enforce these constraints throughout.

2.5 Overall scheme

The workflow of the proposed SIT algorithm is shown in Table 1. After each update of the CS based SIR, an optimization of THT is carried out. In the implementation of the CS based SIR, an alternating minimization algorithm can be adopted. The log-likelihood term is minimized using Eq.(8), while the TV term is minimized using the pseudo inverse of the soft-threshold filtered DGT. The threshold of filtration can be determined adaptively by the projection gradient method[25, 26], which needs an estimate about the true TV. In the optimization of THT, the DBP and corresponding noise variance on each constructed chord should be calculated in advance. An estimate about the uncertainty of DBP can be determined by the variance empirically. The parameter λ is recalculated in each optimization of THT by Eq.(14). After the new THT g^{New} is computed by Eq.(11), an inversion of g^{New} will be carried out by the POCS method. The two alternating operations between the CS based SIR and the optimization of THT will be stopped after a given number of iteration. The final result will be selected after a suitable number of iterations, which can be determined from the λ curves heuristically.

Table 1. The workflow of the proposed SIT.

Initialize: $\mu_0 = 0$;

Construct chords and compute g_s^{DBP} **and** ε_s ;

Set $err_s = \alpha\sqrt{\varepsilon_s}, \quad \alpha = 1$;

Estimate the objective TV.

While

Step 1: CS based SIR

1. **Update image using Eq.(8);**
2. **Determine the threshold using projection gradient method;**
3. **Minimize TV using soft-threshold filtering;**
4. **Obtain the intermediate result** $\tilde{\mu}_t$;

Step 2: Optimization of THT

On each chord:

1. **Compute** g^{Old} **from the intermediate result** $\tilde{\mu}_t$;
2. **Compute the** λ **using Eq.(14);**
3. **Determine** g^{New} **using Eq.(11);**
4. **Inverse** g^{New} **by POCS to update the image;**

Until the stopping criteria is satisfied.

Output the reconstructed result.

3. EXPERIMENTAL RESULTS

A numerical simulation was carried out to validate the proposed SIT approach. A low contrast Shepp-Logan phantom and a fan beam geometry were adopted. The equi-spatial virtual detector was centered at the system origin and made perpendicular to the line from the origin to the x-ray source. The distance from the x-ray source to the system origin was 57 cm. The detector included 360 elements with a total length of 10.8 cm. For a full scan, 360 projections were equi-angularly collected. And 5×10^5 photons per detector element were used to simulate the Poisson projection data. The reconstructed image was in a 256×256 matrix covered a region of radius 10cm. The ROI is an inscribed square inside the FOV formed by the local scanning beam. And chords (PI-lines) were constructed along horizontal direction. On each chord, the ROI covered 96 pixels with a known sub-region of 6 pixels. The phantom was shown in Figure1.

In order to evaluate the estimated noise variance of THT from the measurements, we generated 1000 Poisson projection datasets assuming 5×10^5 photons per detector element. Then, 1000 DBP results calculated from these datasets were used to estimate the empirical noise variance of THT, which was regarded as the evaluation standard. According to Section 2.1, the noise variance of THT can be estimated from the noise variance of the measured line integral data, which is assumed as $\{1/\bar{y}_i\}$. However, $\{1/\bar{y}_i\}$ is unknown in practice. So we adopted $\{1/y_i\}$ to approximate the noise variance of the measured line integral data. In Figure 2, we plotted the noise variances on the chord indicated as "a" in

Figure 1. It can be seen that the noise variance estimated from one-off projection data is similar to the empirical value via 1000 experiments. The variances estimated using $\{1/\bar{y}_i\}$ and $\{1/y_i\}$ were almost the same. Therefore, we can estimate the noise of THT from measurement dataset $\{y_i\}$ in practice.

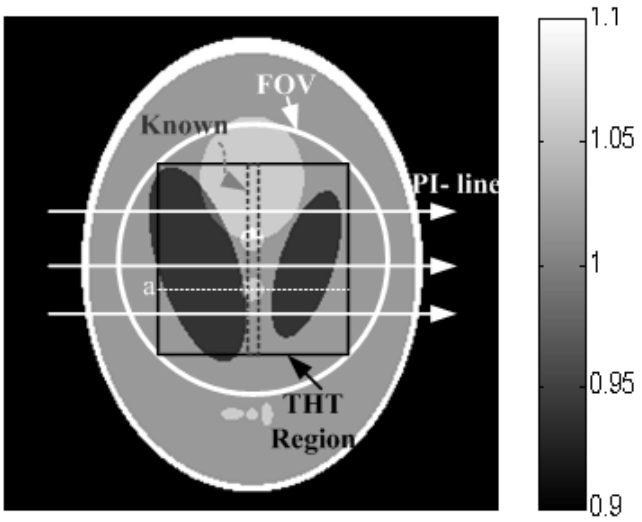

Figure 1. The 2D Shepp-Logan phantom within a display window [0.9 1.1].

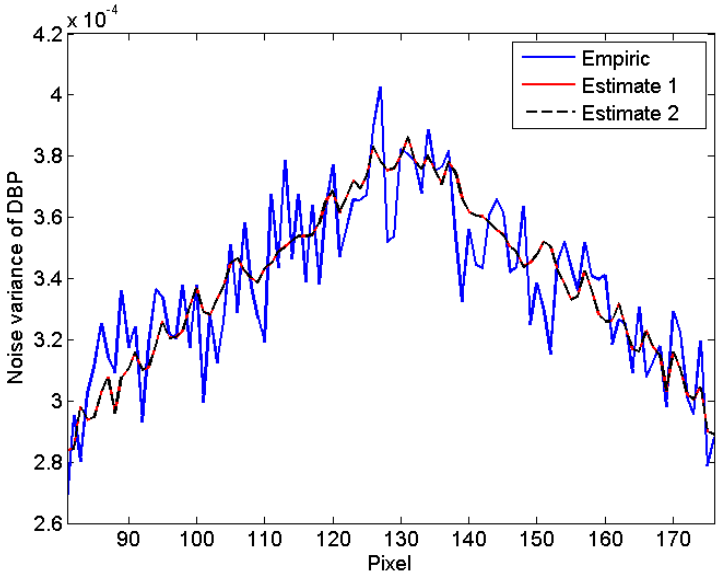

Figure 2. The noise variances of THT on the chord indicated as "a" in Figure 1. The legends "Empiric", "Estimate 1" and "Estimate 2" indicated the results from 1000 experiments, the datasets $\{1/y_i\}$ and $\{1/\bar{y}_i\}$, respectively.

We carried out 50 iterations with the proposed approach. The curves of λ on each chord were shown in Figure 3. It can be seen that the optimal iteration number is not same on each chord. However, we can approximately choose it as 15 iterations. The reconstructed ROI using the proposed SIT after 15 iterations was shown in Figure 4 (a). We compared it with interior tomography approaches. The result by the CS based SIR without a THT constraint was shown in Figure 4(b), the result by the CS based SIR with a noisy THT constraint (just let $g^{New} = g^{DBP}$) was shown in Figure 4(c), and the result by the original THT-based interior tomography (inverse g^{DBP} by POCS) was shown in Figure 4(d). It can be noticed that the proposed approach has the best performance in these interior tomography strategies suppressing noise and bias effectively. The corresponding property demonstrations along the line indicated as "a" in Figure 1 were shown in Figure.5.

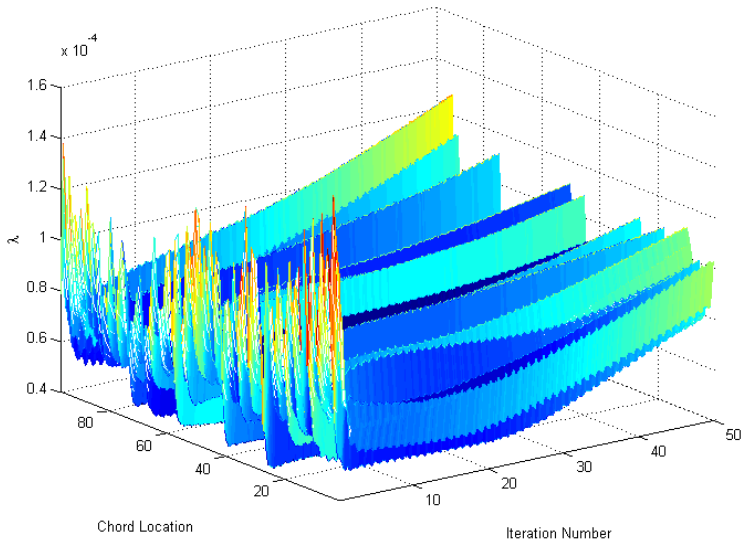

Figure 3. The change curves of λ on each chord.

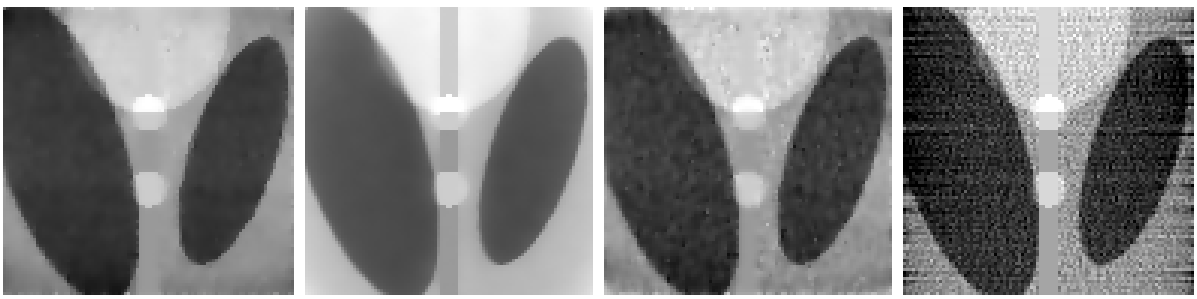

(a) (b) (c) (d)

Figure 4. The reconstructed ROIs. (a) the proposed SIT, (b) the CS based SIR without THT constraint, (c) the CS based SIR with a noisy THT constraint, and (d) the DBP-POCS.

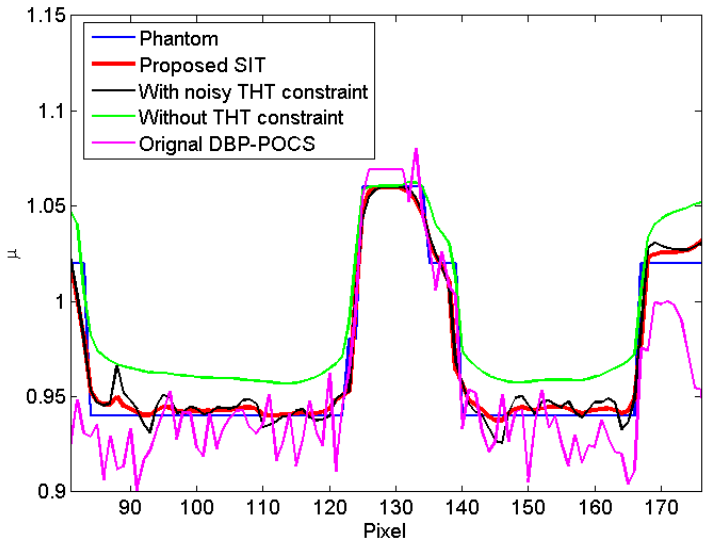

Figure 5. The property demonstrations of the results along the line which is indicated as "a" in Figure 1.

4. DISCUSSIONS AND CONCLUSION

Interior problem is solvable aided by some additional prior information, that is, via inversion of THT with a known sub-region or via CS with a piecewise constant or polynomial ROI. While they are theoretically exact for ideally noiseless data, SIT is in earnest for practical implementation considering the statistical property of projection data in reality. In this paper, we proposed a SIT approach which adds an optimization of THT step after each update of the CS based SIR.

Since the THT computed by the DBP with the measured line integral data is noisy in low-count situation, directly utilizing this noisy THT is sub-optimal, as demonstrated in Figure 4. Therefore, we constructed an objective function to find out an optimal THT taking into account the noise property of the noisy THT. The optimal THT should be close to the noisy THT in probability and also not deviate from the THT of the current reconstruction too much. To make a good balance, we heuristically develop an adaptive method. The idea is based on the fact that the optimal THT should always be in an interval around the noisy THT determined by its variance. Apparently, if the iteration is convergent, the contribution of the noisy THT term will be monotone decreasing. Therefore, we can stop the iteration when the contribution of the noisy THT term decreases slowly or stops decreasing heuristically.

In conclusion, this paper presents a novel SIT approach, which incorporates the THT constraint by an optimizing strategy. On one hand, an optimal THT can be determined statistically from the noisy DBP and the intermediate result from the CS based SIR step. On the other hand, the inversion of the optimized THT will provide an initial image for the next iteration in the CS based SIR step. The optimal iteration number can be determined heuristically by a parameter in optimization of THT. Experiment results show that this method can yield good result with less noise and bias.

ACKNOWLEDGEMENT

This work is partially supported by NSFC (No. 60551003), the program of Chinese Ministry of Education (No. 20060698040, NCET-05-0828), NSF/MRI program (CMMI-0923297), and NIH/NIBIB grant (EB011785).

REFERENCES

[1] Helgason, S., [The radon transform] Birkhauser, (1999).
[2] Louis, A. K., and Rieder, A., "Incomplete data problems in X-ray computerized tomography," Numerische Mathematik, 56(4), 371-383 (1989).
[3] Maass, P., "The interior Radon transform," SIAM Journal on Applied Mathematics, 52(3), 710-724 (1992).
[4] Natterer, F., [The mathematics of computerized tomography] Society for Industrial Mathematics, (2001).
[5] Yu, H. Y., Ye, Y. B., and Wang, G., "Interior tomography: theory, algorithms and applications," Proc. SPIE. 7078, 70780F (2008).
[6] Ye, Y. B., Yu, H. Y., Wei, Y. C. *et al.*, "A general local reconstruction approach based on a truncated Hilbert transform," International Journal of Biomedical Imaging, Article ID:63634, 8 (2007).
[7] Ye, Y. B., Yu, H. Y., and Wang, G., "Exact interior reconstruction with cone-beam CT," International Journal of Biomedical Imaging, Article ID:10693, 5 (2007).
[8] Ye, Y. B., Yu, H. Y., and Wang, G., "Exact interior reconstruction from truncated limited-angle projection data," International Journal of Biomedical Imaging, Article ID:427989, 6 (2008).
[9] Yu, H. Y., Ye, Y. B., and Wang, G., "Interior reconstruction using the truncated Hilbert transform via singular value decomposition," Journal of the X-Ray Science and Technology, 16(4), 243-251 (2008).
[10] Kudo, H., Courdurier, M., Noo, F. *et al.*, "Tiny a priori knowledge solves the interior problem in CT," Physics in Medicine and Biology, 53, 2207-2231 (2008).
[11] Courdurier, M., Noo, F., Defrise, M. *et al.*, "Solving the interior problem of computed tomography using a priori knowledge," Inverse Problems, 24, 065001 (2008).
[12] Noo, F., Clackdoyle, R., and Pack, J. D., "A two-step Hilbert transform method for 2D image reconstruction," Physics in Medicine and Biology, 49, 3903-3923 (2004).
[13] Yu, H. Y., and Wang, G., "Compressed sensing based interior tomography," Physics in Medicine and Biology, 54(9), 2791–2805 (2009).
[14] Yu, H. Y., Yang, J. S., Jiang, M. *et al.*, "Supplemental analysis on compressed sensing based interior tomography," Physics in Medicine and Biology, 54, N425-N432 (2009).
[15] Han, W. M., Yu, H. Y., and Wang, G., "A General Total Variation Minimization Theorem for Compressed Sensing Based Interior Tomography," International Journal of Biomedical Imaging, Article ID:125871, 3 (2009).
[16] Yang, J. S., Yu, H. Y., Jiang, M. *et al.*, "High-order total variation minimization for interior tomography," Inverse Problems, 26, 035013 (2010).
[17] Donoho, D. L., "Compressed sensing," IEEE Transactions on Information Theory, 52(4), 1289-1306 (2006).
[18] Wang, G., Yu, H. Y., and Ye, Y. B., "A scheme for multisource interior tomography," Medical Physics, 36, 3575-3581 (2009).
[19] Xu, Q., Yu, H., Mou, X. *et al.*, "Statistical interior tomography," Proc. SPIE. 7804, 78041I (2010).
[20] Xu, Q., Mou, X., Wang, G. *et al.*, "statistical interior tomography," accepted by IEEE Trans. Med. Imaging.
[21] Zhu, L., Wang, J., and Xing, L., "Noise suppression in scatter correction for cone-beam CT," Medical Physics, 36(3), 741-352 (2009).
[22] Xia, D., Yu, L., Sidky, E. *et al.*, "Noise properties of chord-image reconstruction," IEEE transactions on medical imaging, 26(10), 1328 (2007).
[23] Elbakri, I. A., and Fessler, J. A., "Statistical image reconstruction for polyenergetic X-ray computed tomography," IEEE Transactions on Medical Imaging, 21(2), 89-99 (2002).
[24] Yu, H. Y., and Wang, G., "A soft-threshold filtering approach for reconstruction from a limited number of projections," Physics in Medicine and Biology, 55, 3905-3916 (2010).
[25] Daubechies, I., Fornasier, M., and Loris, I., "Accelerated projected gradient method for linear inverse problems with sparsity constraints," Journal of Fourier Analysis and Applications, 14(5), 764-792 (2008).
[26] Yu, H., and Wang, G., "SART-type image reconstruction from a limited number of projections with the sparsity constraint," International Journal of Biomedical Imaging, Article ID: 934847, 9 (2010).